

# Isotopic links between atmospheric chemistry and the deep sulphur cycle on Mars

Heather B. Franz<sup>1,2</sup>, Sang-Tae Kim<sup>3</sup>, James Farquhar<sup>2</sup>, James M. D. Day<sup>4</sup>, Rita C. Economos<sup>5</sup>, Kevin D. McKeegan<sup>5</sup>, Axel K. Schmitt<sup>5</sup>, Anthony J. Irving<sup>6</sup>, Joost Hoek<sup>2</sup> & James Dutton III<sup>2</sup>

The geochemistry of Martian meteorites provides a wealth of information about the solid planet and the surface and atmospheric processes that occurred on Mars. The degree to which Martian magmas may have assimilated crustal material, thus altering the geochemical signatures acquired from their mantle sources, is unclear<sup>1</sup>. This issue features prominently in efforts to understand whether the source of light rare-earth elements in enriched shergottites lies in crustal material incorporated into melts<sup>1,2</sup> or in mixing between enriched and depleted mantle reservoirs<sup>3</sup>. Sulphur isotope systematics offer insight into some aspects of crustal assimilation. The presence of igneous sulphides in Martian meteorites with sulphur isotope signatures indicative of mass-independent fractionation suggests the assimilation of sulphur both during passage of magmas through the crust of Mars and at sites of emplacement. Here we report isotopic analyses of 40 Martian meteorites that represent more than half of the distinct known Martian meteorites, including 30 shergottites (28 plus 2 pairs, where pairs are separate fragments of a single meteorite), 8 nakhlites (5 plus 3 pairs), Allan Hills 84001 and Chassigny. Our data provide strong evidence that assimilation of sulphur into Martian magmas was a common occurrence throughout much of the planet's history. The signature of mass-independent fractionation observed also indicates that the atmospheric imprint of photochemical processing preserved in Martian meteoritic sulphide and sulphate is distinct from that observed in terrestrial analogues, suggesting fundamental differences between the dominant sulphur chemistry in the atmosphere of Mars and that in the atmosphere of Earth<sup>4</sup>.

Sulphur isotope analyses were undertaken using sequential chemical extraction from whole-rock meteorite samples followed by dual-inlet isotope ratio mass spectrometry and *in situ* secondary ion mass spectrometry (SIMS). The abundance of sulphur extracted from each fraction is reported in Supplementary Table 1 and illustrated in Extended Data Fig. 1. Isotope data are reported in per mil using  $\delta$  and  $\Delta$  notation (Methods and Supplementary Table 2a) and were normalized to measurements of Cañon Diablo Troilite (CDT). A subset of the data, identified with anomalous sulphur isotopic signatures, is reported in Supplementary Table 2b. Anomalous sulphur isotope effects, which produce mass-independent fractionation (MIF), are those in which isotope selection depends on factors in addition to the classical (mass-dependent) selection rules associated with molecular vibrations, rotations and translations. These effects are typically characterized by significant deviations of  $\Delta^{33}\text{S}$ ,  $\Delta^{36}\text{S}$  or both, but we note that small variations in  $\Delta^{33}\text{S}$  and  $\Delta^{36}\text{S}$  may be produced by mixing or distillation processes involving large (tens of per mil) mass-dependent variation in  $\delta^{34}\text{S}$  (Supplementary Information and Extended Data Fig. 3). The magnitude of  $\Delta^{33}\text{S}$  and the absence of significant  $\delta^{34}\text{S}$  variation in Martian meteorites rule out such mixing and distillation and have led to the suggestion that the Martian signatures reflect a mass-independent effect, attributed to ultraviolet photochemistry<sup>5,6</sup>. We discuss below how the MIF signatures observed

in this study provide insight into processes of assimilation of sulphur into magma during transport (observed in shergottites), processes of assimilation of sulphur salts or sulphur-bearing fluids at the time the flows were emplaced (observed in nakhlites), and in some cases processes that introduce MIF sulphur signatures through secondary alteration processes on Mars.

The shergottites are igneous rocks that lack evidence of extensive secondary mineralization<sup>7</sup>. We extracted acid-volatile sulphur (AVS, predominantly monosulphide) from shergottites representing each mineralogical and trace element category identified in the literature. The isotopic composition of the AVS fraction reveals uniformity among these samples (Fig. 1) and establishes a baseline for interpretation of Martian sulphur isotopic data. The weighted mean of analyses yields  $-0.17 \pm 0.11\text{‰}$  for  $\delta^{34}\text{S}$ ,  $0.009 \pm 0.001\text{‰}$  for  $\Delta^{33}\text{S}$  and  $0.02 \pm 0.19\text{‰}$  for  $\Delta^{36}\text{S}$  (see Methods for details; uncertainties represent 2 s.e.m.). The data do not follow a normal distribution and yield a standard deviation of  $0.013\text{‰}$  for  $\Delta^{33}\text{S}$ , which is  $\sim 1.5$  times that predicted from analytical uncertainty alone. The variability in  $\Delta^{33}\text{S}$  for the sample population suggests augmentation by sulphur with anomalous  $\Delta^{33}\text{S}$  that did not originate in the mantle. However, the  $\Delta^{33}\text{S}$  of the mean is tightly constrained and close to the value measured for CDT and bulk chondritic sulphur (average,  $0.002 \pm 0.005\text{‰}$  (s.e.m.)  $\pm 0.025\text{‰}$  (s.d.); refs 8, 9). Data for groups of enriched versus depleted shergottites and mafic versus ultramafic shergottites are distributed about the mean, and the sulphur isotopic composition of Y980459, which is one of the most primitive shergottites and is thus inferred to represent Martian mantle composition<sup>10</sup>, notably lies close to the mean. Although other processes may have influenced the sulphur isotopic composition of shergottites, the mean value of  $0.009\text{‰}$  provides a reasonable measure of the juvenile  $\Delta^{33}\text{S}$  of Mars. This signal is less  $^{33}\text{S}$ -enriched than those observed in some achondrite groups and minor components of chondrites that have been interpreted to reflect heterogeneity in planetary precursor materials<sup>9,11,12</sup>. The variability in  $\Delta^{33}\text{S}$  of Martian sulphur, chondritic sulphur<sup>8,9</sup> and terrestrial mantle sulphur<sup>13</sup> is less than  $0.01\text{‰}$ , implying that sulphur was well mixed in the most abundant inner Solar System materials. The  $\delta^{34}\text{S}$  values derived from our shergottite AVS data are also homogeneous and yield a mean value within error of the CDT value, suggesting efficient mixing in the Martian mantle and little or no fractionation of sulphur isotopes during core formation.

Three shergottites have resolvable mass-independent AVS  $\Delta^{33}\text{S}$  compositions, shown with open symbols in Fig. 1a. These are NWA 2990, NWA 5960 (paired with the former) and Los Angeles, with  $\Delta^{33}\text{S}$  values of  $0.063 \pm 0.014\text{‰}$ ,  $0.093 \pm 0.008\text{‰}$  and  $0.054 \pm 0.008\text{‰}$ , respectively. Because MIF sulphur signatures are not produced by magmatic processes, these observations suggest that sulphur was fractionated by ultraviolet photochemistry in the Martian atmosphere<sup>5,6</sup>, deposited onto the surface and ultimately assimilated into melts, where it was reduced and incorporated into igneous sulphides. NWA 2990, NWA 5960 and Los Angeles also exhibit trace element and radiogenic isotopic characteristics

<sup>1</sup>Center for Research and Exploration in Space Science and Technology, NASA Goddard Space Flight Center, Greenbelt, Maryland 20771, USA. <sup>2</sup>Department of Geology and Earth System Science Interdisciplinary Center, University of Maryland, College Park, Maryland 20742, USA. <sup>3</sup>School of Geography and Earth Sciences, McMaster University, Hamilton, Ontario L8S 4K1, Canada. <sup>4</sup>Scripps Institution of Oceanography, University of California San Diego, La Jolla, California 92093, USA. <sup>5</sup>Department of Earth and Space Sciences, University of California, Los Angeles, California 90095, USA. <sup>6</sup>Department of Earth and Space Sciences, University of Washington, Seattle, Washington 98195, USA.

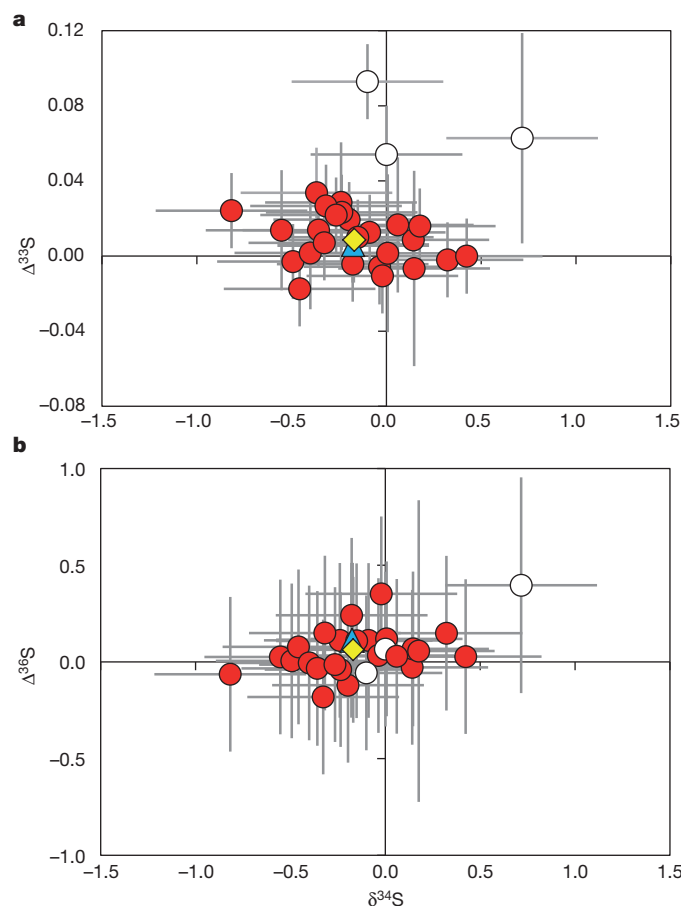


**Figure 1 | Sulphur isotopic compositions of shergottite AVS.** **a**,  $\Delta^{33}\text{S}$  versus  $\delta^{34}\text{S}$ ; **b**,  $\Delta^{36}\text{S}$  versus  $\delta^{34}\text{S}$ . Yellow diamond, weighted mean composition; blue triangle, Y980459; filled circles, samples included in the weighted mean; open circles, samples not included in the weighted mean due to anomalous signatures. Error bars, 2 s.d.

that some workers have interpreted to indicate incorporation of crustal material<sup>14–17</sup>. The coincidence of anomalous sulphide with other geochemical characteristics, including evidence for crystallization under relatively oxidizing conditions<sup>14–17</sup>, suggests a link between anomalous sulphur in igneous minerals and assimilation of crustal material into the melts.

Chemical extractions of sulphide (AVS, chromium-reducible sulphur or both) from Nakhla<sup>5,6</sup> ( $\Delta^{33}\text{S} = -0.08\text{‰}$ ), Allan Hills (ALH) 84001 ( $\Delta^{33}\text{S} = -0.072 \pm 0.008\text{‰}$ ), and Miller Range (MIL) 03346 and three of its pairs ( $\Delta^{33}\text{S} = -0.434 \pm 0.008\text{‰}$  to  $-0.538 \pm 0.008\text{‰}$ ) reveal MIF sulphur signatures (Fig. 2), suggesting that crustal material was assimilated by their parent melts. SIMS analyses of Nakhla pyrrhotite yielded a mean  $\Delta^{33}\text{S}$  value within error of chemical extraction analyses, and SIMS analyses of MIL 03346 pyrrhotite yielded a mean  $\Delta^{33}\text{S}$  value of  $-0.72 \pm 0.13\text{‰}$  (Supplementary Table 3), which is slightly more negative than is observed in chemical extractions. Furthermore, analyses of  $\Delta^{33}\text{S}$  for individual grains of MIL 03346 ranged from  $-0.30 \pm 0.13\text{‰}$  to  $-1.11 \pm 0.13\text{‰}$ , representing a level of variation outside the range of analytical uncertainty, which we interpret to reflect real differences in isotopic composition.

MIL 03346 is an unusual, fast-cooled nakhlite possessing skeletal iron oxide grains and interspersed sulphide in the mesostasis<sup>18</sup> (Fig. 3 and Extended Data Figs 4–6), offering a rare perspective on the petrogenesis of its anomalous pyrrhotite. The heterogeneous, non-zero  $\Delta^{33}\text{S}$  of pyrrhotite grains in MIL 03346 suggests a non-equilibrium process associated with assimilation of sulphur salts during emplacement of the magmatic flow from which this meteorite was derived. Assimilation may also be reflected in the highly oxidized state of this meteorite, because reduction of one mole of S(VI) to S(II) consumes eight moles of electrons and has the potential to oxidize eight moles of Fe(II) to Fe(III). Assimilation of an

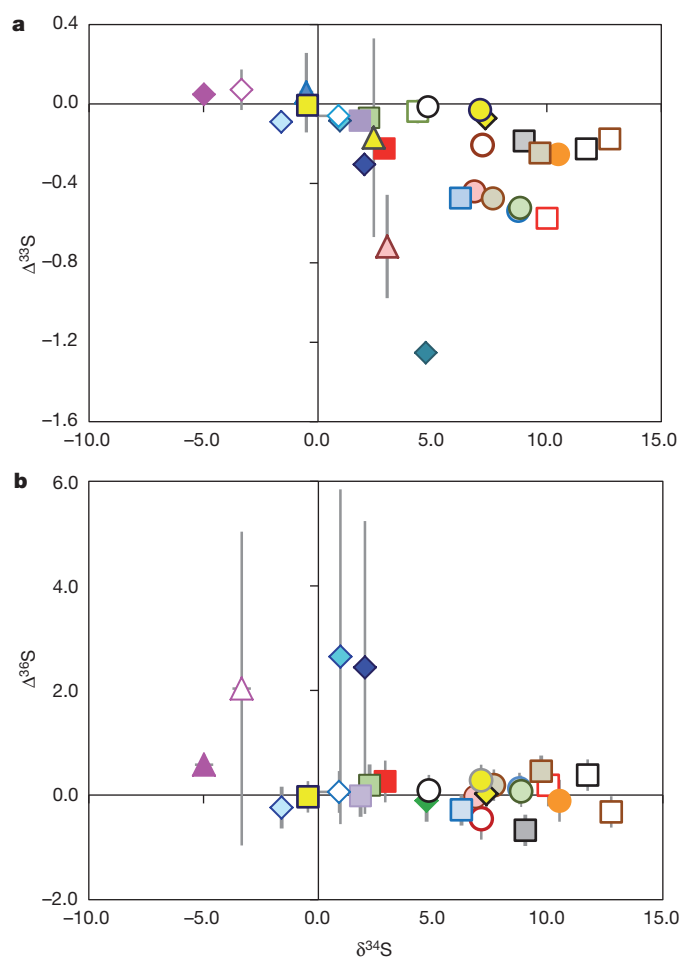


**Figure 2 | Sulphur isotopic compositions of nakhlites and ALH 84001.**

**a**,  $\Delta^{33}\text{S}$  versus  $\delta^{34}\text{S}$ ; **b**,  $\Delta^{36}\text{S}$  versus  $\delta^{34}\text{S}$ . AVS, acid-volatile sulphur; CRS, chromium-reducible sulphur; WSS, water-soluble sulphate; otherwise (no suffix in key), acid-soluble sulphate. Error bars, 2 s.d. Results of previous studies<sup>5,6</sup> are shown for comparison. **a** also includes weighted mean values for SIMS analyses of Nakhla, MIL 03346 and ALH 84001.

oxoanion salt such as sulphate, which would lead to iron loss from pyroxene and formation of magnetite and sulphide, is consistent with both the abundance of iron oxide (magnetite) in MIL 03346 and the variable  $\Delta^{33}\text{S}$  observed in its sulphide minerals. We interpret the differences in  $\Delta^{33}\text{S}$  observed in pyrrhotites of MIL 03346 and Nakhla to reflect local differences in the proportion and sulphur isotopic composition of assimilated sulphate.

ALH 84001 yielded two pyrite grains with  $\Delta^{33}\text{S}$  anomalies, one of which was resolvable at the 2 s.d. level. The remaining grains showed mass-dependent isotopic composition, producing a weighted mean  $\Delta^{33}\text{S}$  of  $-0.17 \pm 0.13\text{‰}$ . As described above, monosulphides of ALH 84001 possess a MIF signature, suggesting assimilation of crustal sulphur into the parent magma. However, pyrite in ALH 84001 is of secondary origin<sup>19,20</sup>. Variations in  $\delta^{34}\text{S}$  and  $\Delta^{33}\text{S}$  observed in pyrite grains by SIMS are consistent with previous reports of sulphur isotopic variability in pyrite from

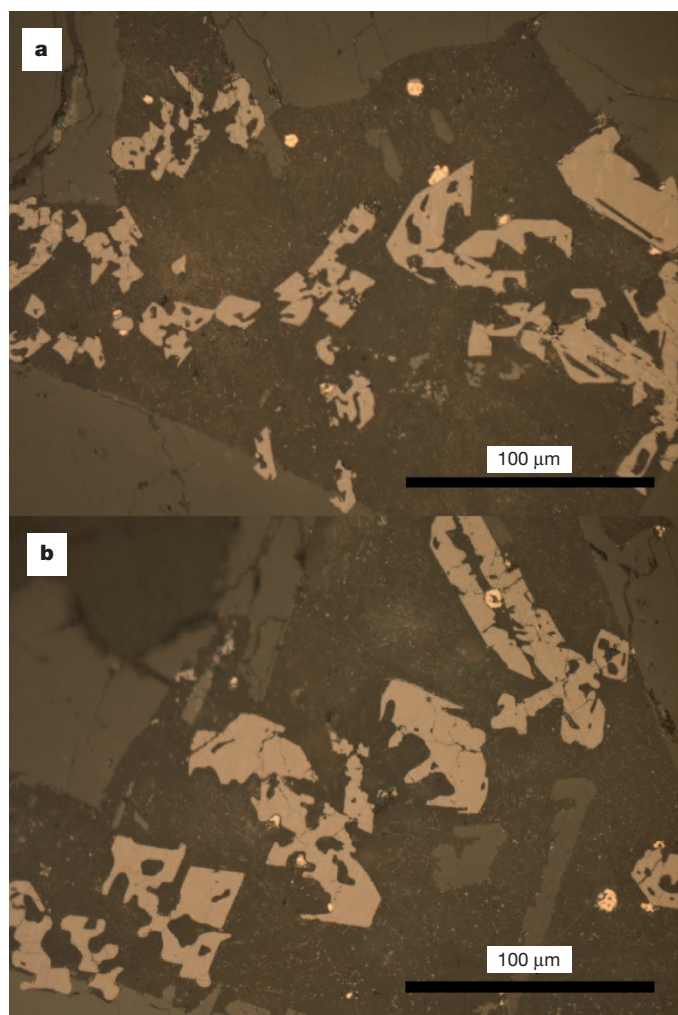


**Figure 3** | Reflected-light images of MIL 090030, paired with MIL 03346. The images illustrate the association between pyrrhotite (bright yellow) and skeletal magnetite (light grey) grains in the intercumulus matrix.

this meteorite<sup>20,21</sup>. There is no evidence that the analysed grains are in brecciated or fragmented zones. Instead, we observed close association of the sulphides with Cr-spinel and maskelynite, as reported in ref. 19. These pyrites have sulphur-poor compositions (Supplementary Table 4), suggesting a possible origin in incomplete sulphurization of igneous pyrrhotite by hydrothermal fluid bearing crustal-derived sulphur—a second mechanism for imparting heterogeneous MIF sulphur isotopic signatures to the meteorites.

Sulphate fractions of the meteorites (Fig. 2) reveal another facet of the Martian sulphur cycle. Anomalous sulphate was detected in six shergottites, Chassigny and all nakhlites analysed. Whereas replicate analyses of NWA 5298 revealed positive  $\Delta^{33}\text{S}$  ( $0.146 \pm 0.008\text{‰}$  and  $0.170 \pm 0.008\text{‰}$ ) in sulphate but insufficient AVS for accurate isotope ratio measurements, the  $\Delta^{33}\text{S}$  signals in sulphate from NWA 2990, NWA 5960 and Los Angeles are within analytical uncertainty of their respective sulphide  $\Delta^{33}\text{S}$  values, suggesting a genetic link between sulphate and sulphide fractions. This sulphate could reflect incomplete chemical reduction of assimilated crustal sulphate within the magma or an origin as a subsequent sulphide oxidation product. In contrast, sulphates from two other shergottites (NWA 5718 and LAR 06319, with  $\Delta^{33}\text{S} = 0.260 \pm 0.008\text{‰}$  and  $0.057 \pm 0.008\text{‰}$ , respectively) and Chassigny ( $\Delta^{33}\text{S} = 0.033 \pm 0.008\text{‰}$ ), which do not have sulphide with anomalous  $\Delta^{33}\text{S}$ , suggest that mass-independent sulphate with positive  $\Delta^{33}\text{S}$  was introduced through post-crystallization aqueous alteration rather than during the magmatic stage.

Similarly, the MIF signature in nakhlite sulphate suggests a combination of sulphate introduced through post-crystallization aqueous alteration and sulphate assimilated by melts. Analyses of sulphate from Nakhla yield  $\Delta^{33}\text{S}$  values as negative as  $-1.25 \pm 0.01\text{‰}$  (ref. 6). Sulphates of MIL 03346 (and pairs), Y000593, NWA 6148 and NWA 998 have sulphur isotopic characteristics consistent with Nakhla, with  $\Delta^{33}\text{S}$  ranging from  $-0.038 \pm 0.030\text{‰}$  to  $-0.576 \pm 0.008\text{‰}$  and  $\Delta^{36}\text{S}$  near zero. Correlating  $\Delta^{33}\text{S}$  with the relative positions of the nakhlites in a cumulate pile formed by gravitational settling of crystals within a magmatic flow<sup>18,22–25</sup> shows that meteorites with the largest negative  $\Delta^{33}\text{S}$  magnitudes (Nakhla, MIL 03346 and Y000593) derive from intermediate depths and that the smallest values of  $\Delta^{33}\text{S}$  are seen in meteorites from the greatest and shallowest depths (NWA 998 and NWA 6148). The variations in sulphate  $\Delta^{33}\text{S}$  among the nakhlites imply differences in composition of their alteration fluids.

Different scenarios have been proposed for nakhlite secondary alteration, including alteration by a single event (see, for example, ref. 26) or by multiple events (see, for example, ref. 27). Multiple events could have introduced fluids characterized by different  $\Delta^{33}\text{S}$  values. Evidence that the Lafayette meteorite experienced alterations unique among the nakhlites, including positive  $\Delta^{33}\text{S}$  anomalies in its sulphate and pyrite<sup>5</sup>, supports the case for multiple events. Although sulphur isotope heterogeneity may be simpler to explain by multiple alteration events, these data do not uniquely support that scenario. Petrological models proposing that the nakhlites were formed by multiple magmatic events instead of a single lava flow (see, for example, refs 23, 28, 29) would assert different constraints on the timing and mode of alteration (Supplementary Information) and are also permitted by the sulphur isotope data.

The data presented here provide insight into the architecture of the Martian sulphur cycle, suggesting the presence of a persistent process that produced geographically distributed sulphur with anomalous  $\Delta^{33}\text{S}$ . Geographical variations in sulphur isotopic composition are supported by different ejection ages of groups of Martian meteorites, indicating that a number of distinct impact events launched meteorites from various locations on the Martian surface (see, for example, ref. 30). The variation in  $\Delta^{33}\text{S}$  with an absence of significant anomalies in  $\Delta^{36}\text{S}$  (Fig. 4) implies MIF production by different pathways from those that operated on the early Earth and in Earth's stratosphere today<sup>4,31</sup>. Furthermore, the positive  $\Delta^{33}\text{S}$  signal in shergottites, Chassigny and Lafayette contrasts the negative  $\Delta^{33}\text{S}$  observed in the other nakhlites and ALH 84001. This variation in  $\Delta^{33}\text{S}$  could indicate a shift in composition of the Martian

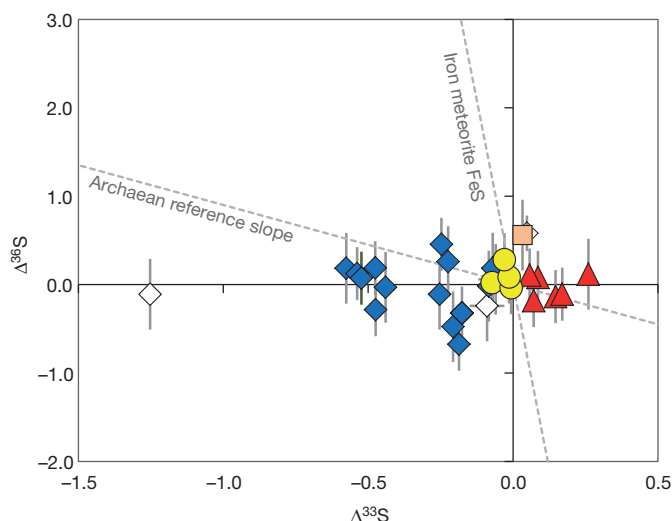


**Figure 4** | Covariation between  $\Delta^{33}\text{S}$  and  $\Delta^{36}\text{S}$  in different groups of Martian meteorites. Diamonds, nakhlites; circles, ALH 84001; triangles, shergottites; square, Chassigny. Martian meteorite data from other studies are included<sup>5,6</sup> (open symbols). Dashed lines depict arrays formed by Archaean terrestrial samples and iron meteorite FeS for comparison. (See Extended Data Fig. 2 for details.) Error bars, 2 s.d.



atmosphere or in the speciation of sulphur-bearing volcanic gases over time, or it could reflect complementary sulphur products generated by a single photochemical process, as suggested by the uniform array formed by the isotopic signatures of these meteorites in the  $\Delta^{36}\text{S}$ – $\Delta^{33}\text{S}$  space.

The prevalence of sulphur extracted as sulphate implies the predominance of sulphate-formation pathways in the generation or preservation, or both, of MIF sulphur on Mars. Evidence for the transfer of sulphate with anomalous  $\Delta^{33}\text{S}$  to the regolith is present in meteorites with a variety of protolith ages (ALH 84001, the nakhlites, Chassigny and six shergottites), suggesting that production of mass-independent signatures was sustained throughout much of Mars' history. Assimilation of sulphate with anomalous  $\Delta^{33}\text{S}$  by Martian melts also seems to have been a common occurrence, as evidenced by isotopic anomalies in sulphide extracted from ALH 84001, several nakhlites and three shergottites (NWA 2990, NWA 5960 and Los Angeles), as well as the small  $\Delta^{33}\text{S}$  variability in the population of shergottites. These observations imply the cycling of sulphur between the regolith and magma that erupted at, or near, the Martian surface.

Anomalous sulphur transferred from surface materials into Martian igneous minerals provides a sensitive marker for crustal assimilative processes, but the absence of a MIF signal in igneous sulphides does not constitute evidence for the absence of assimilation. For example, the composition of light rare-earth elements in early-trapped melt inclusions in LAR 06319 is similar to that in whole rock, indicating that this meteorite probably derived its enrichment properties from partial melting of an enriched and oxidized mantle reservoir, which did not involve assimilation of crustal material<sup>32</sup>. Although this interpretation is in accord with our evidence that MIF sulphur was added to LAR 06319 during post-crystallization alteration, the sulphur isotope ratios cannot rule out assimilation of crustal sulphur that did not bear a MIF signature. Considered in conjunction with data for other isotopic systems and trace element characteristics, sulphur isotope systematics present a powerful tool for reconstructing the geological history of Mars.

## METHODS SUMMARY

A sequential chemical extraction procedure was used to obtain sulphur isotope ratios for different mineral phases in powdered whole-rock samples. Each sample powder was pre-treated by sonicating in Milli-Q water to extract water-soluble sulphate, which was converted to barium sulphate and dried for later reduction. The sample powder was then processed with a series of three acidic solutions to extract different sulphur-bearing phases. In the first step, the sample was heated with 5 N HCl under flowing  $\text{N}_2$  gas. AVS in the sample, presumed to consist primarily of monosulphides, reacted with the HCl to produce  $\text{H}_2\text{S}$  gas, which was collected in an acidic capture solution containing  $\text{AgNO}_3$ . In two subsequent steps, additional reduction solutions were injected into the boiling flask for sequential extraction of acid-soluble sulphate and chromium-reducible sulphur from the sample.

The  $\text{H}_2\text{S}$  produced in each step of the extraction process reacted with  $\text{AgNO}_3$  in the capture solution to form  $\text{Ag}_2\text{S}$ , which was rinsed with Milli-Q water and a 1 M  $\text{NH}_4\text{OH}$  solution, and then dried. Samples of  $\text{Ag}_2\text{S}$  were reacted with  $\sim 10$ -fold stoichiometric excess of pure  $\text{F}_2$  at  $\sim 250^\circ\text{C}$ . Product  $\text{SF}_6$  was purified by both cryogenic and gas chromatographic techniques, and sulphur isotope abundances were measured by monitoring mass/charge ratios  $m/z$  127, 128, 129 and 131 ( $^{32}\text{SF}_5^+$ ,  $^{33}\text{SF}_5^+$ ,  $^{34}\text{SF}_5^+$  and  $^{36}\text{SF}_5^+$ , respectively) with a ThermoFinnigan MAT 253 mass spectrometer. Uncertainties were estimated from repeated measurements of International Atomic Energy Agency reference standards and CDT, and are generally less than 0.15‰, 0.008‰ and 0.15‰ (1 s.d.) for  $\delta^{34}\text{S}$ ,  $\Delta^{33}\text{S}$  and  $\delta^{36}\text{S}$ , respectively. Data were normalized to measurements of CDT.

**Online Content** Any additional Methods, Extended Data display items and Source Data are available in the online version of the paper; references unique to these sections appear only in the online paper.

**Received 4 September 2013; accepted 14 February 2014.**

- Jones, J. H. Isotopic relationships among the shergottites, the nakhlites, and Chassigny. *Proc. Lunar Planet. Sci. Conf.* **19**, 465–474 (1989).
- Herd, C. D. K., Borg, L. E., Jones, J. H. & Papike, J. J. Oxygen fugacity and geochemical variations in the Martian basalts: implications for Martian basalt petrogenesis and the oxidation state of the upper mantle of Mars. *Geochim. Cosmochim. Acta* **66**, 2025–2036 (2002).
- Borg, L. E., Nyquist, L. E., Taylor, L. A., Wiesmann, H. & Shih, C.-Y. Constraints on Martian differentiation processes from Rb–Sr and Sm–Nd isotopic analyses

- of the basaltic shergottite QUE 94201. *Geochim. Cosmochim. Acta* **61**, 4915–4931 (1997).
- Farquhar, J., Bao, H. & Thieme, M. Atmospheric influence of Earth's earliest sulfur cycle. *Science* **289**, 756–758 (2000).
- Farquhar, J., Savarino, J., Jackson, T. L. & Thieme, M. H. Evidence of atmospheric sulphur in the Martian regolith from sulphur isotopes in meteorites. *Nature* **404**, 50–52 (2000).
- Farquhar, J., Kim, S.-T. & Masterson, A. Implications from sulfur isotopes of the Nakhla meteorite for the origin of sulfate on Mars. *Earth Planet. Sci. Lett.* **264**, 1–8 (2007).
- McSween, H. Y. What we have learned about Mars from SNC meteorites. *Meteoritics* **29**, 757–779 (1994).
- Gao, X. & Thieme, M. H. Isotopic composition and concentration of sulfur in carbonaceous chondrites. *Geochim. Cosmochim. Acta* **57**, 3159–3169 (1993).
- Rai, V. K. & Thieme, M. H. Mass independently fractionated sulfur components in chondrites. *Geochim. Cosmochim. Acta* **71**, 1341–1354 (2007).
- Mikouchi, T. et al. Yamato 980459: mineralogy and petrology of a new shergottite-related rock from Antarctica. *Antarct. Meteorite Res.* **17**, 13–34 (2004).
- Gao, X. & Thieme, M. H. Systematic study of sulfur isotopic composition in iron meteorites and the occurrence of excess  $^{33}\text{S}$  and  $^{36}\text{S}$ . *Geochim. Cosmochim. Acta* **55**, 2671–2679 (1991).
- Rai, V. K., Jackson, T. L. & Thieme, M. H. Photochemical mass-independent sulfur isotopes in achondritic meteorites. *Science* **309**, 1062–1065 (2005).
- Labidi, J., Cartigny, P. & Moreira, M. Non-chondritic sulphur isotope composition of the terrestrial mantle. *Nature* **501**, 208–211 (2013).
- Gross, J. et al. Petrography, mineral chemistry, and crystallization history of olivine-phyric shergottite NWA 6234: a new melt composition. *Meteorit. Planet. Sci.* **48**, 854–871 (2013).
- Irving, A. J., Herd, C. D. K., Gellissen, M., Kuehner, S. M. & Bunch, T. E. Paired fine-grained, permafic olivine-phyric shergottites Northwest Africa 2990/5960/6234/6710: trace element evidence for a new type of Martian mantle source or complex lithospheric assimilation process. *Meteorit. Planet. Sci.* **46**, A108 (2011).
- Rubin, A. E. et al. Los Angeles: the most differentiated basaltic Martian meteorite. *Geology* **28**, 1011 (2000).
- Warren, P. H., Greenwood, J. P. & Rubin, A. E. Los Angeles: a tale of two stones. *Meteorit. Planet. Sci.* **39**, 137–156 (2004).
- Day, J. M. D., Taylor, L. A., Floss, C. & McSween, H. Y. Jr. Petrology and chemistry of MIL 03346 and its significance in understanding the petrogenesis of nakhlites on Mars. *Meteorit. Planet. Sci.* **41**, 581–606 (2006).
- Mittlefehdt, D. W. ALH 84001, a cumulate orthopyroxene member of the Martian meteorite clan. *Meteoritics* **29**, 214–221 (1994).
- Greenwood, J. P., Mojzsis, S. J. & Coath, C. D. Sulfur isotopic compositions of individual sulfides in Martian meteorites ALH 84001 and Nakhla: implications for crust-regolith exchange on Mars. *Earth Planet. Sci. Lett.* **184**, 23–35 (2000).
- Shearer, C. K., Layne, G. D., Papike, J. J. & Spilde, M. N. Sulfur isotopic systematics in alteration assemblages in Martian meteorite Allan Hills 84001. *Geochim. Cosmochim. Acta* **60**, 2921–2926 (1996).
- Mikouchi, T., Miyamoto, M., Koizumi, E., Makishima, J. & McKay, G. Relative burial depths of nakhlites: an update. *Proc. Lunar Planet. Sci. Conf.* **37**, abstr. 1865 (2006).
- Jambon, A. et al. Northwest Africa 5790. Top sequence of the nakhlite pile. *Proc. Lunar Planet. Sci. Conf.* **41**, 1696 (2010).
- Mikouchi, T. & Miyamoto, M. Comparative cooling rates of nakhlites as inferred from iron-magnesium and calcium zoning of olivines. *Proc. Lunar Planet. Sci. Conf.* **31**, abstr. 1343 (2002).
- Udry, A., McSween, H. Y., Lecumberri-Sanchez, P. & Bodnar, R. J. Paired nakhlites MIL 090030, 090136, and 03346: insights into the Miller Range parent meteorite. *Meteorit. Planet. Sci.* **47**, 1575–1589 (2012).
- Bridges, J. C. & Grady, M. M. Evaporite mineral assemblages in the nakhlite (Martian) meteorites. *Earth Planet. Sci. Lett.* **176**, 267–279 (2000).
- Halls, L. J. & Taylor, G. J. Comparisons of the four Miller Range nakhlites, MIL 03346, 090030, 090032 and 090136: textural and compositional observations of primary and secondary mineral assemblages. *Meteorit. Planet. Sci.* **46**, 1787–1803 (2011).
- Shirai, N. & Ebihara, M. Chemical characteristics of nakhlites: implications to the geological setting for nakhlites. *Proc. Lunar Planet. Sci. Conf.* **39**, 1643 (2008).
- Shih, C.-Y., Nyquist, L. E., Reese, Y. & Jambon, A. Sm–Nd isotopic studies of two nakhlites, NWA 5790 and Nakhla. *Proc. Lunar Planet. Sci. Conf.* **41**, 1367 (2010).
- McSween, H. Y. in *The Martian Surface: Composition, Mineralogy, and Physical Properties* (ed. Bell, J. F.) 383–396 (Cambridge Univ. Press, 2008).
- Baroni, M., Savarino, J., Cole-Dai, J., Rai, V. K. & Thieme, M. H. Anomalous sulfur isotope compositions of volcanic sulfate over the last millennium in Antarctic ice cores. *J. Geophys. Res.* **113**, D20112 (2008).
- Basu Sarbadhikari, A., Day, J. M. D., Liu, Y., Rumble, D. & Taylor, L. A. Petrogenesis of olivine-phyric shergottite Larkman Nunatak 06319: implications for enriched components in Martian basalts. *Geochim. Cosmochim. Acta* **73**, 2190–2214 (2009).

**Supplementary Information** is available in the online version of the paper.

**Acknowledgements** We acknowledge the Meteorite Working Group, L. Welzenbach, T. McCoy, S. Ralew, M. N. Rao, L. Nyquist, J. Zipfel, C. Smith, H. Kojima, A. Treiman,

T. Bunch and B. Zanda for providing meteorite samples analysed in this study. We also thank P. Piccoli for assistance with electron microprobe analyses. The manuscript benefited from independent reviews by M. Thiemens, P. Cartigny, S. Ono, D. Johnston and B. Wing during revision. The UCLA ion microprobe facility is partly supported by a grant from the US National Science Foundation Instrumentation and Facilities Program. This work was supported by NASA Cosmochemistry grants NNX09AF72G and NNX13AL13G to J.F.

**Author Contributions** H.B.F. and J.F. designed the study and wrote the manuscript. All authors contributed to data collection, data interpretation and editing the manuscript.

**Author Information** Reprints and permissions information is available at [www.nature.com/reprints](http://www.nature.com/reprints). The authors declare no competing financial interests. Readers are welcome to comment on the online version of the paper. Correspondence and requests for materials should be addressed to H.B.F. ([heather.b.franz@nasa.gov](mailto:heather.b.franz@nasa.gov)).

## METHODS

**Acid-based chemical extraction procedures.** The most precise laboratory technique for measuring sulphur isotope ratios involves the conversion of all sulphur-bearing phases to  $\text{SF}_6$ , which removes the potential for isobaric interference during mass spectrometric analysis<sup>33,34</sup>. This study was performed with a sequential chemical extraction procedure on powdered whole rock that allowed the measurement of sulphur isotope ratios for different mineral phases. Meteorite samples were received either as rock chips or already powdered. Samples of shergottites, Y000593, NWA 6148 and NWA 998 received as rock chips were disaggregated in a steel mortar and then ground more finely with an agate mortar and pestle. Each powdered sample was transferred to a 15-ml centrifuge tube along with 10 ml of Milli-Q water. The tube was sonicated for 20 min to promote the dissolution of water-soluble sulphate from the sample. The tube was then centrifuged to allow separation of the solution from the solid sample by pipette. This process was repeated to yield a total of 20 ml of solution containing water-soluble sulphate, which was transferred to a boiling flask. A few drops of 0.5 N HCl were added to the flask to reduce the pH to  $\sim 3$ , followed by several drops of 1 M  $\text{BaCl}_2$  solution to precipitate any sulphate in the solution as  $\text{BaSO}_4$ . The flask was then allowed to evaporate to dryness before the sulphate was reduced by a procedure similar to that described below for acid-soluble sulphate.

The powdered sample was transferred from the centrifuge tube to a double-necked boiling flask with a silicone septum. The flask was assembled with a water-cooled condenser, a bubbler filled with Milli-Q water, and a sulphide trap into a distillation apparatus similar to that described in ref. 35. All ground-glass joints were sealed with PTFE sleeves. The apparatus was assembled, checked for leaks and then purged with nitrogen for at least 10 min. For the first extraction step, 25 ml of 5 N HCl was injected into the boiling flask through the septum with a syringe. The solution was then heated to  $\sim 60^\circ\text{C}$ . AVS in the sample, presumed to consist primarily of monosulphides, reacted with the HCl to evolve  $\text{H}_2\text{S}$  gas, which was captured in an acidic  $\text{AgNO}_3$  solution. After completion of the AVS reduction reaction ( $\sim 3$  h), the sulphide trap with capture solution was replaced and 25 ml of a reduction solution prepared from 12 N hydrochloric acid, 48% hydriodic acid and 50% hypophosphorus acid (a 'Thode solution'<sup>36,37</sup>) were added to the boiling flask. The solution was heated to  $\sim 85^\circ\text{C}$ . During the next 4.5 h, acid-soluble sulphate in the sample reacted to form  $\text{H}_2\text{S}$ , which was captured in the manner described above.

At this point, two slightly different techniques were used to extract the final sulphur-bearing fraction. For all but the last three shergottites analysed (NWA 7032, NWA 7042 and Tissint), on completion of the acid-soluble sulphur reduction, the sulphide trap was again replaced with fresh  $\text{AgNO}_3$  solution. An acidic Cr(II) solution (15 ml) was injected into the boiling flask containing the AVS and Thode solution, which had already been heated to  $\sim 85^\circ\text{C}$ . During the next  $\sim 3$  h, CRS minerals were converted to  $\text{H}_2\text{S}$  and captured in the  $\text{AgNO}_3$  solution. Pyrrhotite, the most common monosulphide mineral in the Martian meteorites, is in general readily extracted in the AVS fraction, but extractions of terrestrial pyrrhotite-rich basalts<sup>38</sup> and nakhlites (this study) suggest that some sulphur-rich pyrrhotite compositions are unreactive to 5 N HCl and instead contribute to the CRS fraction. The CRS fraction also would include any disulphide minerals and elemental sulphur present in the sample.

The sulphur isotope ratios for the shergottite CRS fractions obtained with the above procedure showed an anomalous pattern of depletion in  $^{34}\text{S}$  and enrichment in  $^{33}\text{S}$ , prompting the concern that complex chemical reactions had occurred between the Thode and CRS solutions to produce isotopically biased CRS results. For this reason, the following modified procedure was used to extract the CRS fraction from Chassigny, Y000593, NWA 6148, NWA 998, NWA 7032, NWA 7042 and Tissint. On completion of the acid-soluble sulphate reduction, the boiling flask was cooled and its contents were transferred to 30-ml centrifuge tubes. After separation of the acid solution from the solid sample powder, the sample was rinsed with Milli-Q water several times to clean it before being transferred back to the double-necked boiling flask. The following day, the distillation apparatus was reassembled, checked for leaks and again purged with nitrogen for 10 min. A fresh sulphide trap with  $\text{AgNO}_3$  capture solution was installed. For the final reduction step, 15 ml of the CRS solution and 15 ml of 5 N HCl was injected into the boiling flask, which was then heated to  $\sim 85^\circ\text{C}$ , converting CRS in these samples to  $\text{H}_2\text{S}$  and capturing it in  $\text{AgNO}_3$  solution, as previously described.

The  $\text{H}_2\text{S}$  evolved in each step of the extraction process reacted with the  $\text{AgNO}_3$  in the capture solution to form  $\text{Ag}_2\text{S}$ , which was cleaned with Milli-Q water and 1 M  $\text{NH}_4\text{OH}$  solution, and then dried. The  $\text{Ag}_2\text{S}$  was converted to  $\text{SF}_6$  by reaction with 250  $\mu\text{mol}$  of fluorine gas in a nickel reaction vessel at  $250^\circ\text{C}$  for 8 h. The  $\text{SF}_6$  was subsequently condensed from the residual  $\text{F}_2$  into a trap cooled with liquid nitrogen. Excess  $\text{F}_2$  was passivated by reaction with KBr salt. Replacement of the liquid nitrogen coolant on the trap with ethanol slush at  $-115^\circ\text{C}$  allowed distillation of the  $\text{SF}_6$  from the trap into the liquid-nitrogen-cooled injection loop of a

gas chromatograph. The  $\text{SF}_6$  was purified using a 1/8-inch-diameter, 6-foot-long Molecular Sieve 5A gas chromatograph column and then a 1/8-inch-diameter, 12-foot-long Haysep-Q gas chromatograph column. Both columns were held at  $50^\circ\text{C}$ , with a helium carrier gas flow rate of  $20\text{ ml min}^{-1}$ . After its elution from the gas chromatograph, the  $\text{SF}_6$  was captured in spiral glass traps cooled with liquid nitrogen, and then transferred to the bellows of a ThermoFinnigan MAT 253 dual-inlet gas source mass spectrometer. The sulphur isotopic composition of the  $\text{SF}_6$  was measured by monitoring  $\text{SF}_5^+$  ion beams at  $m/z$  of 127, 128, 129 and 131.

Sulphur isotope ratios are reported in standard  $\delta$  notation with respect to CDT, where  $\delta^{34}\text{S} = [(^{34}\text{S}/^{32}\text{S})_{\text{sample}} / (^{34}\text{S}/^{32}\text{S})_{\text{CDT}} - 1] \times 1,000\text{‰}$ ,  $\Delta^{33}\text{S} = (^{33}\text{S}/^{32}\text{S})_{\text{sample}} / (^{33}\text{S}/^{32}\text{S})_{\text{CDT}} - [(^{34}\text{S}/^{32}\text{S})_{\text{sample}} / (^{34}\text{S}/^{32}\text{S})_{\text{CDT}}]^{0.515}$  and  $\Delta^{36}\text{S} = (^{36}\text{S}/^{32}\text{S})_{\text{sample}} / (^{36}\text{S}/^{32}\text{S})_{\text{CDT}} - [(^{34}\text{S}/^{32}\text{S})_{\text{sample}} / (^{34}\text{S}/^{32}\text{S})_{\text{CDT}}]^{1.9}$ . Uncertainties, estimated from repeated analyses of the sulphur isotopic ratios of IAEA reference materials, are generally less (in magnitude) than 0.15‰, 0.008‰ and 0.15‰ (1 s.d.) for  $\delta^{34}\text{S}$ ,  $\Delta^{33}\text{S}$  and  $\Delta^{36}\text{S}$ , respectively.

Several samples were excluded from calculations of the weighted mean for shergottite AVS isotopic composition. As discussed in the main text, three shergottites were found to possess MIF sulphur isotopic compositions in their AVS fractions (NWA 2990, NWA 5960 and Los Angeles) and were excluded from weighted mean calculations for  $\delta^{34}\text{S}$ ,  $\Delta^{33}\text{S}$  and  $\Delta^{36}\text{S}$ , because they seem to carry an anomalous sulphur-bearing component distinct from the primary shergottite signature. In addition, only data for samples with  $\text{SF}_6$  pressure  $\geq 1$  Torr were included in the mean for  $\Delta^{36}\text{S}$ . All samples that were excluded from  $\Delta^{36}\text{S}$  mean calculations are indicated in Supplementary Tables 1 and 2a.

Samples of MIL 03346 and ALH 84001 were disaggregated in a steel mortar and then ground more finely with an agate mortar and pestle. Each powdered sample was transferred to a 15-ml centrifuge tube along with 10 ml of Milli-Q water. The tube was sonicated for 30 min to promote the dissolution of water-soluble sulphate from the sample. The tube was then centrifuged to allow separation of the solution from the solid sample by pipette. This process was repeated to yield a total of 20 ml of solution containing water-soluble sulphate, which was transferred to a boiling flask before the sulphate was reduced by a procedure similar to that described below for acid-soluble sulphate.

The powdered sample was transferred from the centrifuge tube to a double-necked boiling flask with a silicone septum. The flask was assembled with a water-cooled condenser, a bubbler filled with Milli-Q water, and a sulphide trap into a distillation apparatus as described above. All ground-glass joints were sealed with PTFE sleeves. The apparatus was assembled, checked for leaks and then purged with nitrogen for 10 min. For the first extraction step, 20 ml (25 ml for ALH 84001) of 5 N HCl was injected into the boiling flask through the septum with a syringe. The solution was then heated to  $\sim 60^\circ\text{C}$  to reduce AVS in the sample to  $\text{H}_2\text{S}$ , which was captured in an acidic  $\text{AgNO}_3$  solution. After 3 h, the first sulphide trap and bubbler were replaced with a new trap and bubbler containing fresh silver nitrate solution and fresh Milli-Q water, respectively, and the reaction was continued for 30 min for MIL 03346 and  $\sim 4$  h for ALH 84001. After the second sulphide trap and the bubbler were removed and replaced with a new trap and a bubbler filled with fresh Milli-Q water, 15 ml of acidic  $\sim 0.3$  M Cr(II) solution was then injected into the hot boiling flask ( $\sim 60^\circ\text{C}$ ) and the reaction was allowed to proceed for a total of 4 h for the extraction of CRS. After 3 h, the third sulphur trap and the bubbler were removed and a new sulphur trap and a bubbler were used for the remaining 1 h of the reduction. Again, after a new sulphur trap and a bubbler were introduced, 20 ml of Thode solution (see above) was injected into the hot boiling flask for the reduction of acid-soluble sulphate. During the course of heating ( $\sim 85^\circ\text{C}$ ) and purging with nitrogen ( $\sim 40$  h), the sulphide trap and the bubbler were changed seven times (five times for ALH 84001) for a new trap containing fresh silver nitrate trapping solution and Milli-Q water, respectively.

The  $\text{H}_2\text{S}$  evolved in each step of the extraction process reacted with the  $\text{AgNO}_3$  in the capture solution to form  $\text{Ag}_2\text{S}$ , which was subsequently cleaned, dried and fluorinated in the manner described in the preceding section for ultimate determination of sulphur isotope ratios.

Samples of MIL 090030, MIL 090032 and MIL 090136 were disaggregated in a steel mortar and pestle. Each powdered sample was transferred to a 15-ml centrifuge tube along with 10 ml of Milli-Q water. The tube was sonicated for 30 min to promote the dissolution of water-soluble sulphate from the sample. The tube was then centrifuged to allow separation of the solution from the solid sample by pipette. This process was repeated to yield a total of 20 ml of solution containing water-soluble sulphate, which was transferred to a boiling flask and allowed to evaporate to dryness before the sulphate was reduced by a procedure similar to that described below for acid-soluble sulphate.

The powdered sample was transferred from the centrifuge tube to a double-necked boiling flask with a silicone septum. The flask was assembled with a water-cooled condenser, a bubbler filled with Milli-Q water, and a sulphide trap into a distillation apparatus as described above. All ground-glass joints were sealed with

PTFE sleeves. The apparatus was assembled, checked for leaks and then purged with nitrogen for 10 min. For the first extraction step, 20 ml of 5 N HCl that had been deoxygenated by purging with N<sub>2</sub> was injected into the boiling flask through the septum with a syringe. The solution was then heated to ~60 °C to reduce AVS in the sample to H<sub>2</sub>S, which was captured in an acidic AgNO<sub>3</sub> solution. After completion of the reaction (~3 h), the first sulphide trap and bubbler were replaced with a new trap and bubbler containing fresh silver nitrate solution and fresh Milli-Q water, respectively. An acidic ~0.3 M Cr(II) solution (15 ml) was passed through a 0.2-µm filter and then injected into the hot boiling flask (~60 °C). The reaction was allowed to proceed for 4 h for the extraction of CRS.

On completion of the CRS reduction step, several drops of 1 M BaCl<sub>2</sub> solution were added to the flask to precipitate any sulphate in the solution as BaSO<sub>4</sub>. The contents of the boiling flask were then centrifuged and the CRS solution was decanted. The remaining solids were placed in a single-necked boiling flask with 20 ml of Thode solution as described above. The flask was assembled in the reduction apparatus with a third sulphur trap and bubbler containing fresh Milli-Q water and silver nitrate solution, respectively. The apparatus was then purged under nitrogen flow for 10 min and heated for reduction of acid-soluble sulphate, by a procedure similar to that described in the preceding paragraphs.

The H<sub>2</sub>S evolved in each step of the extraction process reacted with the AgNO<sub>3</sub> in the capture solution to form Ag<sub>2</sub>S, which was subsequently cleaned, dried and fluorinated in the manner described in the preceding section for ultimate determination of sulphur isotope ratios.

**Ion microprobe.** Another technique for measuring multiple sulphur isotopes is SIMS, also known as the ion microprobe. SIMS offers the best spatial resolution for *in situ* analysis of individual mineral grains for measurements of δ<sup>33</sup>S, δ<sup>34</sup>S and Δ<sup>33</sup>S. This method was used to examine sulphides in nakhlites and ALH 84001, with the goal of determining whether the anomalous sulphur isotopic composition obtained from chemical extraction of bulk rock material was also evident in individual grains. Four polished thick sections of Antarctic meteorite MIL 03346 and three polished thin sections of ALH 84001 were obtained from the Meteorite Working Group. Polished thin sections of Nakhla were obtained from the Smithsonian National Museum of Natural History. The SIMS analyses described in this document were performed at the University of California at Los Angeles, using a Cameca IMS 1270 high-resolution ion microprobe in multicollector mode. Polished meteorite samples first were mapped with reflected-light optical microscopy to locate sulphide grains large enough (that is, ~20 µm diameter) for SIMS analysis. Before being loaded in the ion microprobe sample chamber, the sections were cleaned by sonication in Milli-Q water and methanol, and then coated with a ~100 Å layer of gold or carbon to ensure conductivity across the sample surface. Ion microprobe analyses in January 2012 used a 5-nA Cs<sup>+</sup> primary ion beam at 20-keV impact energy with 100-µm Kohler illumination, focused to a 25–30-µm spot. A mass-resolving power of ~4,000 and energy filtering were used to minimize the contributions from the <sup>32</sup>SH<sup>–</sup> ion to the <sup>33</sup>S<sup>–</sup> peak. Positive-charge build-up on the sample was prevented by applying a normal-incidence electron flood gun. Before each analysis, the surface was pre-sputtered for up to 150 s, and this was followed by 30 cycles (60 cycles in some cases) of 10-s integrations. The resulting secondary ions of <sup>32</sup>S<sup>–</sup>, <sup>33</sup>S<sup>–</sup> and <sup>34</sup>S<sup>–</sup> were simultaneously collected using Faraday cups. Measurements of Nakhla in January 2008 employed similar operating conditions to those described above, but with mass resolution of ~6,000.

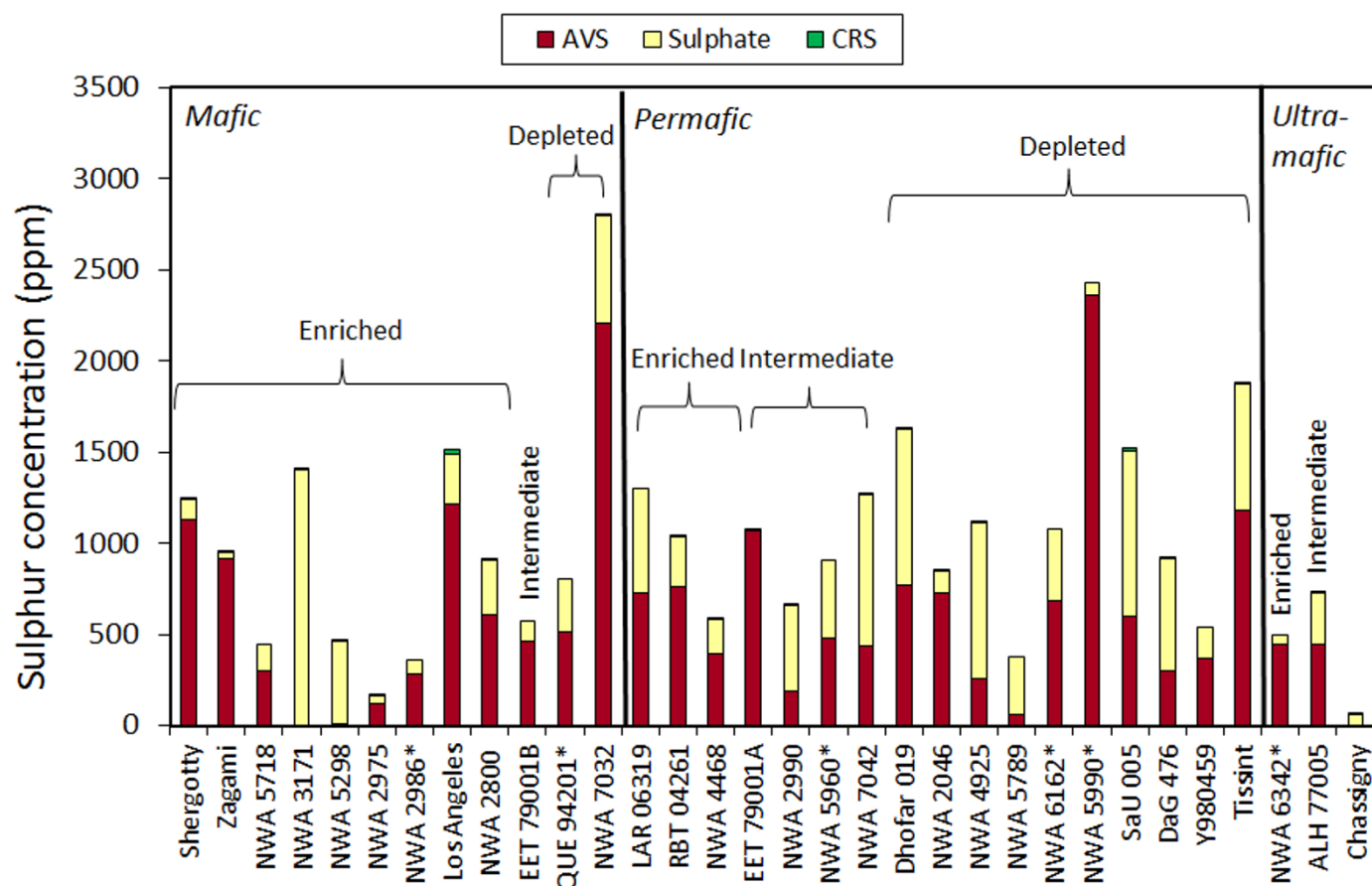
The precision achieved during SIMS analysis is highly dependent on mineral grain and primary beam characteristics, which affect the number of sulphur ions produced. Isotope ratios determined by SIMS also exhibit mass-dependent fractionation, causing deviations from the true isotope ratios that can be predicted and corrected in a systematic manner. The fractionation may be due to the ionization process of sputtering or the transport of secondary ions to the detector, or both. These biases are corrected by calibration with matrix-matched standards under the same instrumental conditions. Note that isotopic fractionations due to matrix effects are solely mass dependent and thus (to first order) do not affect Δ<sup>33</sup>S measurements.

The reported uncertainty in measurements of sulphide grains in the meteorite sections was taken as the greatest of the internal error, the standard error of repeated analyses of mineral standards in the same sessions (that is, the 'external reproducibility') and the standard error of multiple analyses of a given grain. Measurements of MIL 03346, NWA 6148 and ALH 84001 in January 2012 achieved average 1 s.d. precisions of ±0.07‰ for Δ<sup>33</sup>S and ±0.07‰ for δ<sup>34</sup>S, based on repeatability of reference standards. The uncertainty in Δ<sup>33</sup>S measurements of ALH 84001 was a little higher, ±0.25‰, owing to smaller grain sizes. The average 1 s.d. precisions for Nakhla analyses in January 2008 were ±0.04‰ for Δ<sup>33</sup>S and ±0.15‰ for δ<sup>34</sup>S.

**Electron microprobe.** Petrographic and mineralogical characterizations were performed in preparation for ion microprobe analysis. Petrographic analysis and imaging of thin sections were performed using a petrographic microscope equipped with a high-resolution digital camera. Major- and minor-element analyses of sulphide were obtained using a JEOL JXA-8900 SuperProbe (EPMA) with a ZAF correction at the University of Maryland. Wavelength-dispersive spectrometry scans were performed with an accelerating potential of 15 kV and dwell times of 20 s for iron and sulphur and 30 s for the remaining elements. Natural and synthetic standards were used for calibration and were measured periodically within analytical sessions. Drift was within counting error throughout every analytical session. Analyses of MIL 03346 used a 20-nA beam current, and the beam was focused to 2 µm. The detection limits (3 s.d. above background) are <0.01 wt% for all elements listed. Analyses of the remaining meteorites were performed with a beam current of 10 nA and a spot size of 1 µm. The precision of sulphur and iron measurements based on repeated analyses of a pyrrhotite standard during these sessions was approximately 0.2 wt% (1 s.d.).

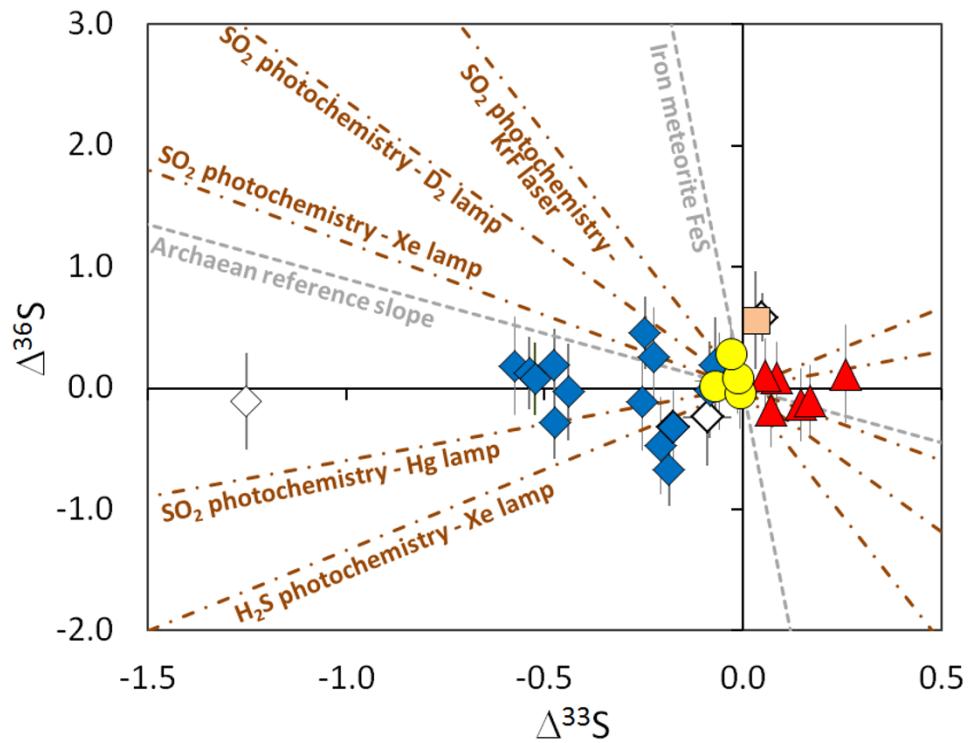
33. Hulston, J. R. & Thode, H. G. Variations in the S<sup>33</sup>, S<sup>34</sup>, and S<sup>36</sup> contents of meteorites and their relation to chemical and nuclear effects. *J. Geophys. Res.* **70**, 3475–3484 (1965).
34. Farquhar, J., Savarino, J., Airieau, S. & Thieme, M. H. Observation of wavelength-sensitive mass-independent sulfur isotope effects during SO<sub>2</sub> photolysis: implications for the early atmosphere. *J. Geophys. Res.* **106**, 32829–32839 (2001).
35. Forrest, J. & Newman, L. Silver-110 microgram sulfate analysis for the short time resolution of ambient levels of sulfur aerosol. *Anal. Chem.* **49**, 1579–1584 (1977).
36. Thode, H. G., Monster, J. & Dunford, H. B. Sulphur isotope geochemistry. *Geochim. Cosmochim. Acta* **25**, 159–174 (1961).
37. Mayer, B. & Krouse, H. R. in *Handbook of Stable Isotope Analytical Techniques* Vol. 1 (ed. de Groot, P.) 538–596 (Elsevier Science, 2004).
38. Labidi, J., Cartigny, P., Birck, J. L., Assayag, N. & Bourrand, J. J. Determination of multiple sulfur isotopes in glasses: a reappraisal of the MORB δ<sup>34</sup>S. *Chem. Geol.* **334**, 189–198 (2012).





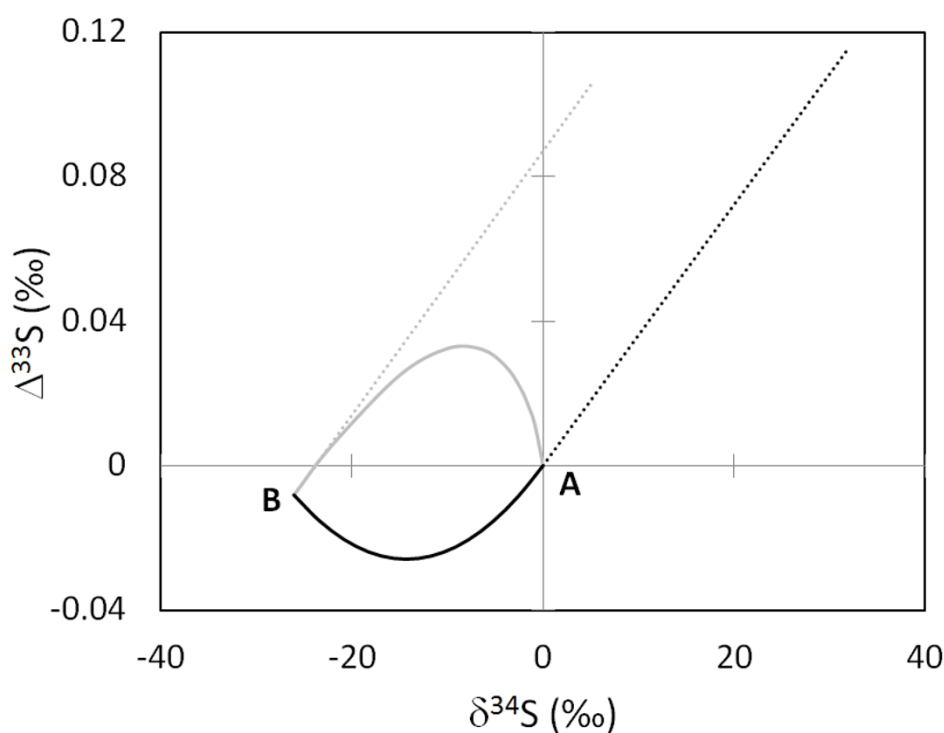
**Extended Data Figure 1 | Sulphur concentrations for shergottites and Chassigny.** Asterisks indicate samples for which not all fractions were recovered. Uncertainty (1 s.d.) is estimated as  $\pm 2\%$  of values.





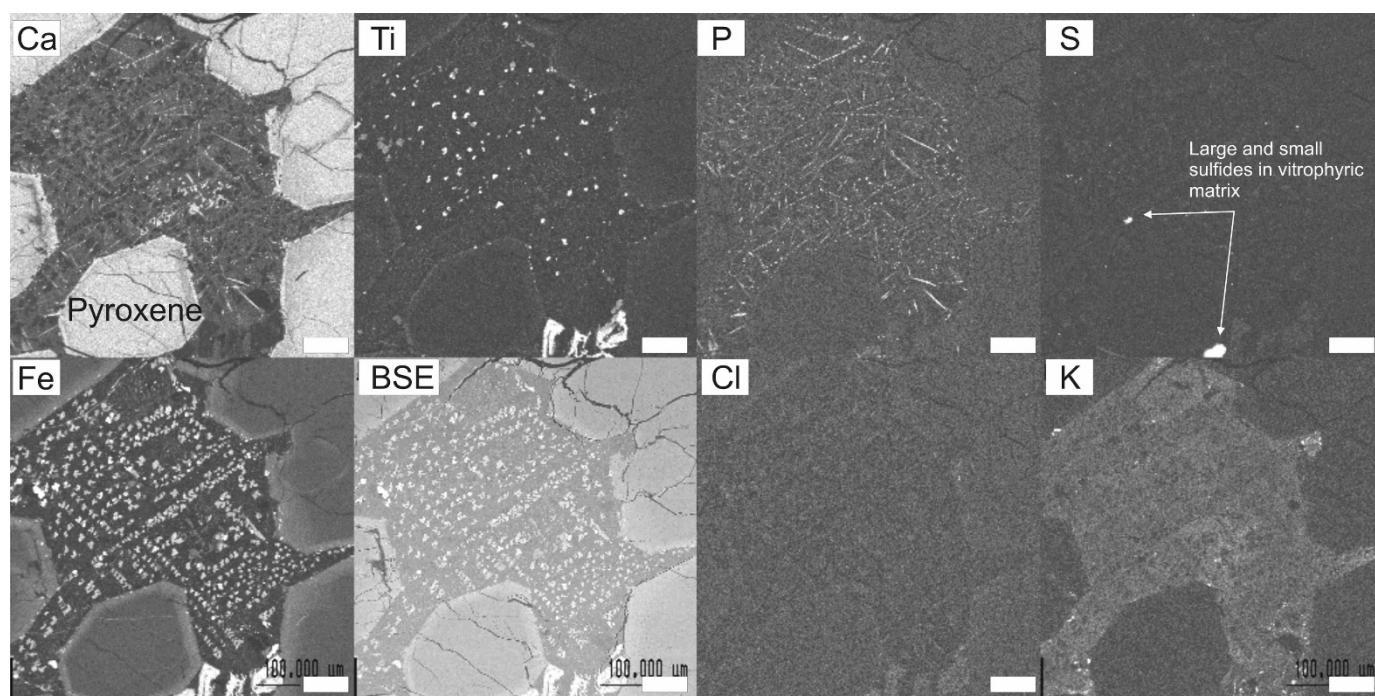
**Extended Data Figure 2 | Covariation between  $\Delta^{33}\text{S}$  and  $\Delta^{36}\text{S}$  in different groups of Martian meteorites, with comparison to iron meteorite FeS, Archaean samples and products of laboratory photochemical experiments accessing different experimental conditions and ultraviolet wavelengths.**

Diamonds, nakhrites; circles, ALH 84001; triangles, shergottites; square, Chassigny. Includes data from other studies: Martian meteorites<sup>5,6</sup>, iron meteorites<sup>11</sup>, Archaean data<sup>4</sup> and photochemistry data (refs 5, 34 and ref. 89 in Supplementary Information).



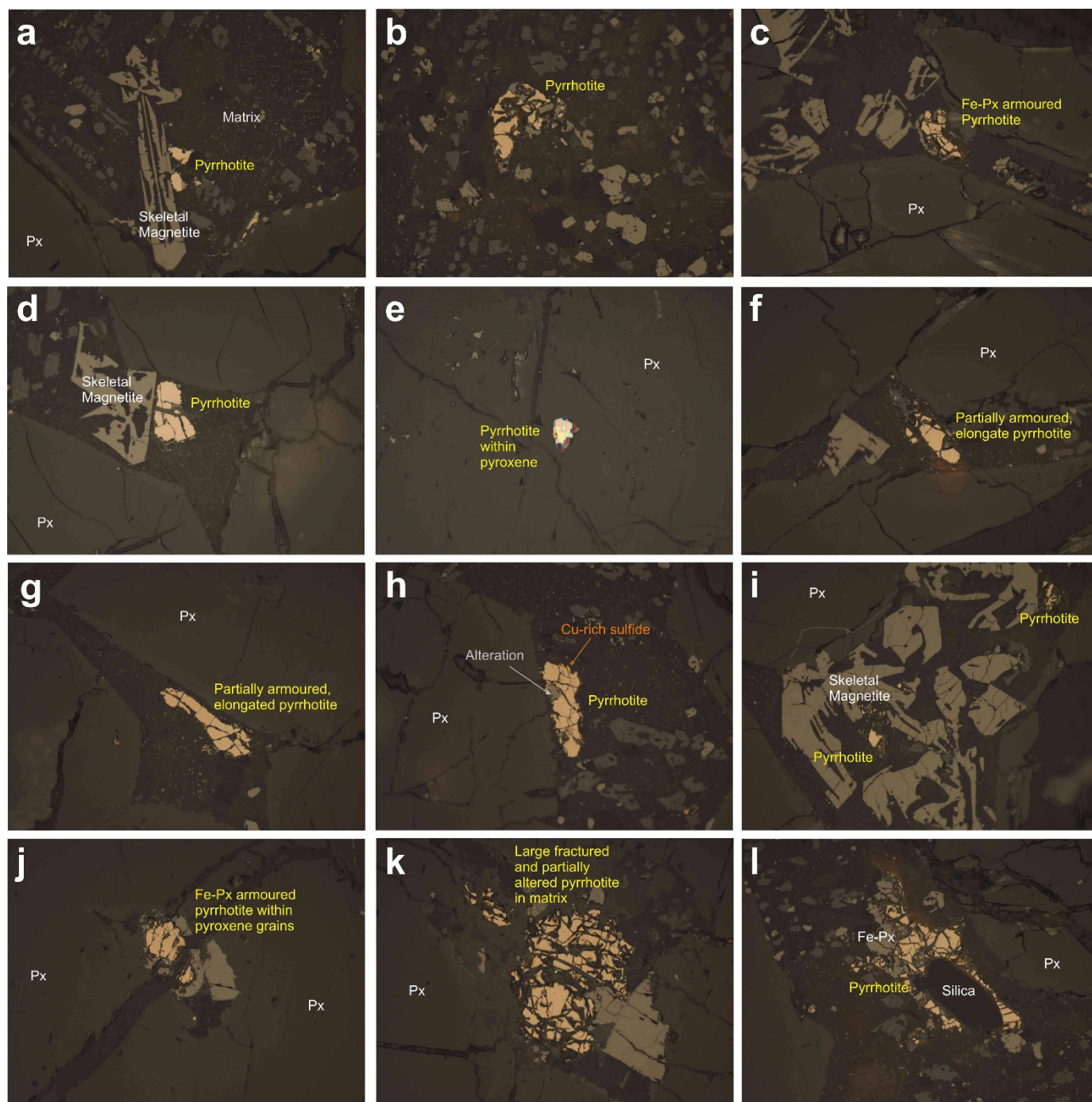
**Extended Data Figure 3 | Plot of  $\Delta^{33}\text{S}$  versus  $\delta^{34}\text{S}$  showing arrays for mixing between compound A and compound B (solid black line), and Rayleigh fractionation with formation of compound B at the expense of compound A.** The dotted black line is the array of compositions formed for residual reactant (A). The dotted grey line is the array of compositions formed for the instantaneous product (B). The solid grey line is the array of compositions formed for the accumulated product (B). The calculations assumed fractionation factors between compound B and compound A of

0.9739409 for  $^{34}\text{S}/^{32}\text{S}$  and 0.9864855 for  $^{33}\text{S}/^{32}\text{S}$ , which are similar to those observed between sulphide and sulphate at 250 °C. This plot illustrates how non-zero  $\Delta^{33}\text{S}$  can be produced by mixing and Rayleigh fractionation involving fractionated endmembers. The scarcity of evidence for highly fractionated  $\delta^{34}\text{S}$  in the data collected for Martian meteorites argues against this process as an origin for the non-zero  $\Delta^{33}\text{S}$  in the nakhlites, and by extension, the other Martian meteorites.



**Extended Data Figure 4 | Back-scattered electron (BSE) image and Ca, Ti, P, S, Fe, Cl and K X-ray maps of MIL 03346, section 118.** Note the fine filaments of phosphate-rich materials and pervasive high-K content of the intercumulus

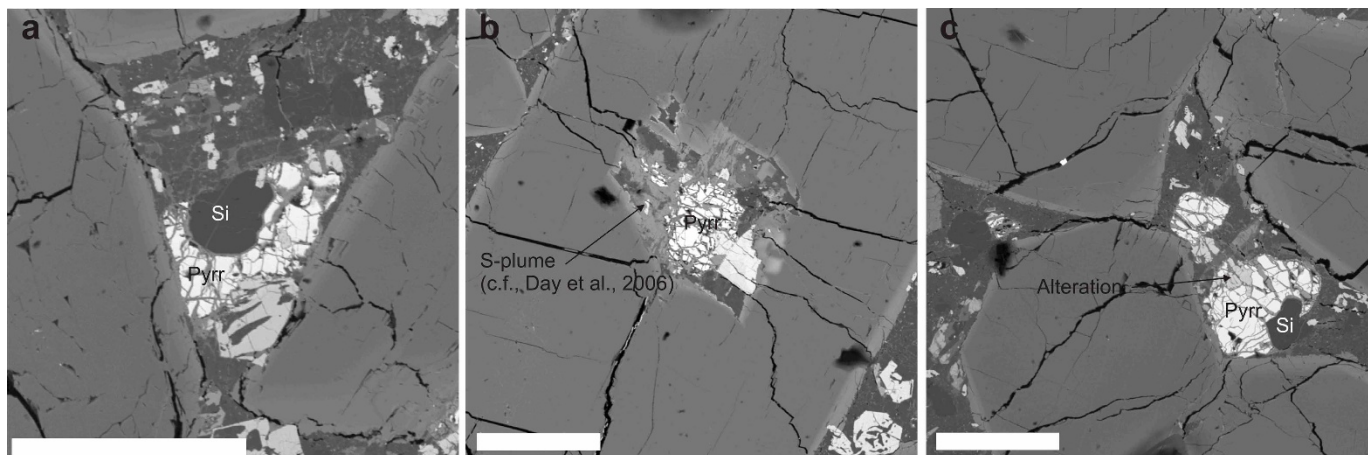
matrix. Sulphides are restricted to the intercumulus matrix and range in size from  $\geq 20 \mu\text{m}$  to  $< 1 \mu\text{m}$ . Scale bars, 100  $\mu\text{m}$ .



**Extended Data Figure 5 | Reflected-light images of representative sulphide grains in MIL 03346, sections 6, 93, 104 and 132.** All images, except **k** and **l** (mag.,  $\times 20$ ), are at  $\times 50$  magnification. Images **a**, **b**, **c**, **f**, **i** and **l** are from

MIL 03346, section 6, and images **d** and **e**, **h** and **k**, and **g** are from MIL 03346, sections 104, 93 and 132, respectively.





**Extended Data Figure 6 | Back-scattered electron images of sulphides in MIL 03346, section 6 (c) and MIL 03346, section 93 (a, b).** Note the fractured appearance of the sulphides and occurrence of Fe(OH) in the cracks and along

the edges of matrix-exposed sulphides, as well as the presence of a sulphate 'plume' in **b**, giving a smoky appearance to the enclosing matrix material. Scale bars, 100  $\mu\text{m}$ .